ANISOTROPIC DAMAGE MODELLING OF COMPOSITE MATERIALS USING ULTRASONIC STIFFNESS MATRIX MEASUREMENTS

A. Paipetis[1,2], Y. Z. Pappas[1], D.E. Vlachos[1] and V. Kostopoulos[1]

[1]Applied Mechanics Laboratory, Dept of Mechanical & Aeronautical Engineering, University of Patras
[2]Marine Materials Technology Dept, Hellenic Naval Academy

ABSTRACT

The monitoring of the elastic properties of Al_2O_3/Al_2O_3 composite material during the exposure at high temperature environment that simulates the working conditions of a gas turbine has been performed non-destructively using ultrasonics. The method is based on velocity measurements of the elastic waves that propagate in an orthotropic medium. These were estimated experimentally using a custom pulser-receiver setup which allows control of the angle of the incident pulse on the sample, while the latter is immersed in a water bath. The derivation of the elastic constants in order to reproduce the stiffness matrix of the composite is an inverse wave propagation problem described by the Christoffel equation. The damage initiation and propagation as depicted by the deterioration of the moduli of the material was described using deterministic and stochastic approaches. Finally, the damage accumulation process was simulated as a Markov process.

1.INTRODUCTION

The unique properties of continuous fibre ceramic matrix composites are attributed to the combination of enhanced structural integrity and high temperature (HT) stability [1,2]. In this way, they offer the best alternative to other exotic materials such as superalloys, which are now very close to their physical limits. The increased high temperature performance, the modular reinforcement design as the tailoring of their microstructure allows their use in high-end applications [3], [4-8].

In this work the performance of Oxide-Oxide (Al_2O_3/Al_2O_3) composites is studied. Oxide-Oxide (Al_2O_3/Al_2O_3) composites offer high temperature stability in oxidising environments up to 1200 ˚C [9]. The study involves the non-destructive evaluation of the stiffness of the composite during thermal loading, simulating the service environment of the composite. The stiffness matrix was constructed using the ultrasonic technique [10, 11]. The procedure is based on the measurement of the time difference for the longitudinal (QL) and one or both transverse waves (QT), and is only valid when the QL and the QT waves are appropriately separated [12]. The subsequent numerical solution of the inverse scattering problem yields the stiffness values [11].

Stiffness properties were monitored in all principal directions in order to monitor anisotropic damage development. This is crucial in materials possessing limited degree of symmetry, such as fibrous composites, as the material anisotropy is expected to change according to the material loading history [13].

Exponential anisotropic damage functions were developed to describe the deterioration of the composite properties [14]. Additionally a stochastic damage accumulation model is employed using Weibull statistics [15] and discrete time Markov chain models to yield service life probability distributions [16]. A Markov process is defined as a process that depends on its current state and its transition to future state and is independent of its past. Finally, a simulation of the degradation path is performed assuming a discrete Markov process with deterministic or stochastic parameters [17].

2. EXPERIMENTAL

2.1 Materials and Methods

The material under investigation in the present study is an improved, compared to former attempts [6], mullite matrix NEXTEL 720 (3000 denier) fibre [7-8] reinforced composite with a fugitive fibre/matrix carbon interface applied by Sol/Gel technique [9]. The material consists of sol-gel carbon fugitive coated 3M Nextel 720 fibers, with a mullite-based matrix. The specimens were 12-layer symmetric cross-ply laminates produced by pyrolysis and infiltration of polymer preforms [9]. The polymer infiltration process (PIP) was employed for the fabrication of the material [10-11]. The composite laminate was made using a symmetric 0°/90° fibre lay-up orientation, with a total fibre volume fraction of 41%.

All specimens were monitored non-destructively and the ultrasonic stiffness matrix measurements were performed in their "as-received" condition. For each specimen the stiffness measurement was repeated at different well-determined regions. Reference specimens were kept out of the high temperature exposure process to be used for the mechanical characterization of the composite at its initial/original state.

Following the high temperature exposure into the special chamber, the same specimens were again tested non-destructively and ultrasonic stiffness matrix measurements were performed once more at the same regions noted above. In that way, it was possible to identify the change in stiffness components for each individual specimen. This approach assists to compensate the inaccuracies of the method and the properties variation within the same test sample.

2.2 Ultrasonic Stiffness Measurements

In the case of an isotropic material only two engineering constants (Young's modulus and Poisson ratio) are sufficient to fully describe its elastic behaviour. These constants can be easily determined from the results of a simple tensile test. When dealing with anisotropic materials, such as composites, nine independent constants are required. These constants are the coefficients of the elasticity tensor that fully describes the elastic behaviour of the material. In this case, conventional mechanical testing can determine directly only part of the elements of the elasticity tensor. However, since elastic wave propagation is directly related to the elastic properties of the medium of propagation, ultrasonic measurements can provide the complete determination of the elasticity tensor of anisotropic materials.

The determination of the elastic properties of anisotropic materials (assumed to be orthotropic in the case of oxide/oxide composites) can be achieved by calculating the coefficients of the propagation equation of an elastic plane wave, based on a set of properly chosen velocity measurements along known material directions. These measurements are carried out using a special experimental setup [18]. Using appropriate signal processing instrumentation, the phase velocities of each of the propagated waves within the specimen are calculated for a number of specimen/probe relative orientations [6-7, 9]. The calculation of the phase velocity is based on the difference between the flight time of each the waves in the presence of the anisotropic material and the flight time of the emitted signal within the coupling fluid without the specimen. The procedure is based on the measurement of the time difference for the longitudinal and one or both transverse waves, and is only valid when the QL and the QT waves are appropriately separated. The numerical solution of the inverse problem by the interpolation of the experimental slowness curves yields the stiffness values [9].

Following this process for the determination of the elements of the stiffness matrix of a given solid at the different stages of its loading life, the evolution of the anisotropic damage formed within the material structure can be traced. This is still possible even in the most extreme case where the ascertained damage alters the initial degree of anisotropy of the loaded material.

2.3 Characterization Procedure

For the purposes of the present study, a detailed testing procedure was planned. A number of test coupons were prepared according to CEN ENV 658-1 and subjected to high temperature exposure for different exposure periods, in the absence of any mechanical loading, into a specially designed chamber that simulates the working environment of a gas turbine. This chamber was actually a furnace producing temperatures up to 1200 ^{o}C, and it was equipped with a system that supplied a gas compound, having the same chemical composition as the combustion gases, simulating the conditions inside a gas turbine combustion chamber.

Each set of specimens corresponding to different exposure duration was subjected to series of tests. Firstly, all the samples were passed through C-scan examination in order to obtain their reference state concerning the quality of the material for each specimen. This was a prerequisite for the initial evaluation of the results of the following tests.

At this stage the ultrasonic stiffness matrix measurements were performed for all the specimens, using the experimental set-up described above. Two Panametric immersion transducers (5 MHz, 15 mm diameter) were used. The frequency was carefully chosen in order to assure wavelengths at least 5 times the dimension of the representative volume element of the material under investigation in the propagation direction and simultaneously to achieve proper separation between the QL and QT waves [12].

For the needs of the present analysis it was assumed that the damage developed during HT exposure does not affect the degree of anisotropy of the material. This means that assuming the starting state of the material is orthotropic, the induced damage does not change its degree of anisotropy, keeping the same principal axes of symmetry. Following the non-destructive ultrasonic tests, the specimens were tested in tension until fracture. The results of these tests are used to derive both modulus of elasticity in the loading direction and the ultimate tensile strength. The results from catastrophic tests performed compared to the results obtained by the ultrasonic technique exhibited excellent agreement [14].

3. RESULTS

The results of the ultrasonic measurements for the deterioration of the moduli E_1, E_2 and E_3 (1 and 2 are the in plane principle directions, with direction 1 associated to the length of the specimen) are shown in fig. 1. The deterioration values are mean values that observed at each specimen, in order to minimise systematic errors. Since the material is a 0/90 symmetric laminate, E_1 and E_2 are expected to be equal. However a difference of about 10% is shown in the results. This can be attributed to edge effects, since the width of the specimen is lower than the length and this results to lower values for the E_2 modulus. In square plates the method yields consistent results, i.e. almost equal E_1 and E_2 values.

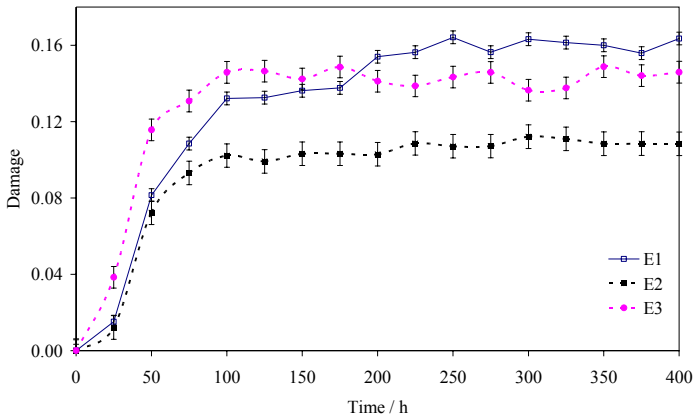

Fig. 1: Damage evolution for E1, E2 and E3: Master curves and standard deviation

The characterization process shows a drop in modulus of up to 16 % for the E_1 modulus, 10 % for the E_2 and 14% E_3 moduli, increasing the exposure duration. It must be stressed that more than a 50% of the stiffness reduction occurs at the first 50 hours of exposure.

4. DISCUSSION

4.1 Deterministic Damage Evolution Modelling

The ultrasonics methodology that has been developed in the previous sections, provides the tool for the non-destructive estimation of the deterioration of the elastic properties of the composite at any stage of its service life. This is made obvious by the accurate estimation of elastic constants of the material at different stages of exposure.

In the case under consideration, the problem lies in expressing the deterioration of the material as a damage function, which is measured at discrete time intervals as deterioration in the stiffness characteristics of the material [13]. Any definition of the damage function has to include this time dependence. The elements of the stiffness matrix are the damage indicators, whereas the stiffness matrix at any discrete time **C** can be written as the algebraic sum of the initial $\mathbf{C}_0$ and a time dependent term $\mathbf{C}_c$ which corresponds to the stiffness loss due to the deterioration of the material [18].

The deterioration for E_1, E_2, E_3 was monitored experimentally. Assuming that there is no coupling, the damage function is identical to the damage function of a scalar quantity for each measured modulus or more specifically:

$$\frac{d\omega}{dt} = A \cdot f^{m}(\sigma,\varepsilon) \cdot (1-\omega)^{-n} \qquad (1)$$

where

ω : the damage function

$f(\sigma,\varepsilon)$: the stress strain state function of the material

A,m,n : material constants

The above equation correlates the time dependence of the damage to a non-linear function of the damage. As a typical case, the rate of damage ($d\omega/dt$) at any time may be

regarded as directly proportional to the damage ω, which corresponds to the simplest form of the damage function:

$$\frac{d\omega}{dt} = A \cdot (1 - \omega) \quad (2)$$

The integral of Eq. (2) is the typical case of exponential reduction which is indicative of a variety of natural processes.

The deterioration of the Young moduli of the material, may be regarded as an exponential reduction process. However, the damage process is not continuing until failure but it is asymptotically approaching a value not greater than 0.16, 0.10 and 0.10 respectively for the three moduli. In this case the deterioration of the material is not continuing until the failure of the material as Eq. (8) suggests, but is asymptotically approaching a value S^{∞}_{11} after which further exposure is not affecting the material. The deterioration function may be defined:

$$R(t) = \frac{E(t) - E_{\infty}}{E_0 - E_{\infty}} \quad (3)$$

where E(t) is the generalised modulus at any given time t corresponding to the inverse of the diagonal elements of the compliance tensor and E_0 and E_{∞} are the initial and final modulus values. The deterioration function at any given time t is $1 \leq R(t) \leq 0$ and by definition is R(t)=1-ω. In this case Eq. (19) becomes:

$$\frac{dR}{dt} = A \cdot R(t) \quad (4)$$

Integrating Eq. (21) for boundary conditions ω=0 for t=0:

$$R(t) = e^{-At} \quad (5)$$

Equivalently, the damage function is:

$$D(t) = 1 - e^{-At} \quad (6)$$

As a result, the problem of defining the damage function for the thermal exposure of the composite, is simplified to the experimental definition of a set of exponential constants $1/\omega_{\infty}$ for the diagonal components of the compliance matrix as well as the value E^{∞}_{i} as they may be calculated from the experimental measurements with the ultrasonics method. In fig. 2 the interpolated damage function for E_1 and E_3 is shown.

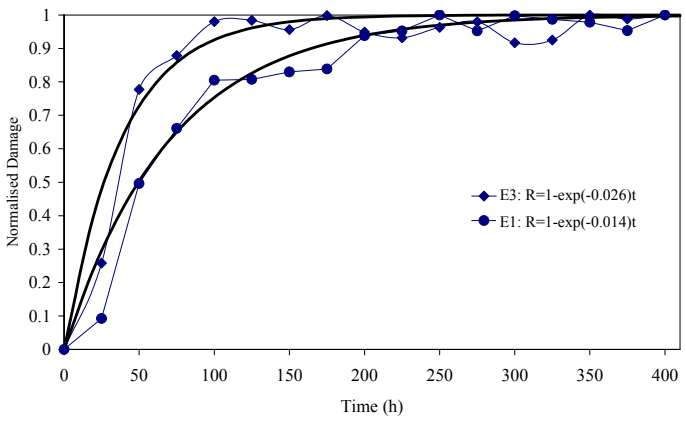

Fig. 2: Damage evolution for E_1 & E3: Normalised function and experimental data

4.2 Stochastic Damage Modelling

For the statistical representation of the results, the data where sorted and classified in 14 classes depending on the span of the experimental distributions. The number of hits in each class represents the cumulative probability function for each constant and each level of loading. The experimental cumulative distributions are shown in fig. 3 for E_3.

The distributions for all three constants exhibit similar dispersion and the characteristic sigmoidal shape, as is expected in life probability distributions. The increase of exposure time leads to the displacement of the distributions without any notable change in their qualitative characteristics. This is attributed to the nature of the loading, which is different from the typical fatigue case where the experimental scatter is expected to increase with loading cycles. As should be mentioned, the particular loading scenario does not allow the model application in time scale for life prediction monitoring, as the experimental monitoring of the composite properties is performed at discrete time intervals, and life expectancy is arbitrarily defined as the value where the measured quantity is leading asymptotically.

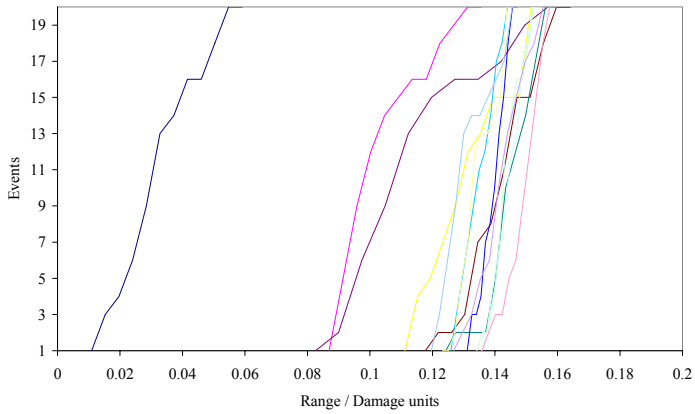

Fig. 3: Damage evolution for E3: Cumulative distributions for all levels of exposure

4.2.1 Weibull Statistics

The representation of the experimental cumulative density functions can be performed regarding the experimental cumulative density function as the cumulative probability of failure P(f). The probability that an elastic constant is within the class *i* is:

$$P(f) = i/n+1 \quad (7)$$

where *i* is the class index and n the number of events within the class. If the function is a Weibul distribution function, the failure probability is:

$$P(f) = 1-(e^{(-V_t(c_f/c_0)^m)}) \quad (8)$$

where V_t is the characteristic volume, c_f a constant for the discrete level of exposure, c_0 the shape parameter and m the scale parameter. For unit volume of statistical observation, which coincides with the sampling volume of the interrogating ultrasonic beam V_t=1, the distribution parameters may be defined experimentally through the linear interpolation of the following equation:

$$ln(C_f)=1/m\ (ln\ (ln\ (P(f)^{-1})\ +\ ln\ (C_0))) \quad (9)$$

The typical Weibull interpolation is shown in fig. 4. The scale parameter corresponds to the characteristic volume damage which can be defined as σ_0^*:

$$\sigma_0^* = \sigma_0/[-V_t]^{1/m} \quad (10)$$

The Weibull distribution function is simulating a non-stationary damage accumulation process which is a special case of a non stationary Poisson process [15].

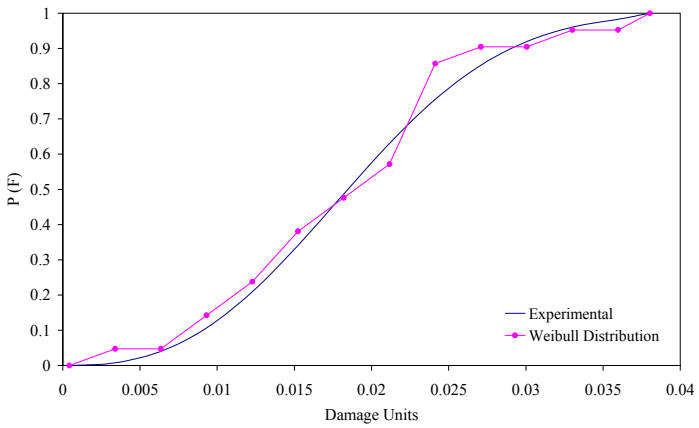

Fig. 4: Characteristic Weibull regression for a random observation state

4.2.2 Markov Process Modelling

The damage accumulation process can be represented as a "shock" process. The shock process is indicated in the specific case as the experimental measurement protocol which is discrete and can be regarded as a discrete Markov process.

According to the shock model [15,16,17], the damage accumulation process is discrete, that is partitioned in finite operating time spans (duty cycles, DC) where damage accumulation is observed. In this way, time scale is discrete. Typical processes of this type are on-off operations, load-unload, lifting cycles etc. In the specific case, the experimental protocol is a stop-and-go which rendering the time dimension discrete. At the same time, it was assumed that damage is discrete $d=1,2,3,\ldots b$, and the final stage b corresponds to failure or the need for replacement. As already stated, the normalized damage is asymptotically leading to a value which is assumed to correspond to "failure". As should be noted, damage is increasing monotonically with exposure (or that the probability of "negative damage" is zero). This assumption enforces the separate modeling of each specimen. All stated assumptions are equivalent to the representation of damage process as a discrete process.

Assuming that for x=0 damage is in stage 1, and that during 1 duty cycle a shock is occurring. If this shock leads to measurable damage, then damage goes to stage 2 and if not it remains in stage 1. The probability of the shock to be beneath a critical level with a given amount of damage in stage 1 is p_1 and the probability to be above a critical level is q_1=1-p_1. If there is a series of Bernoulli trials until the critical value is achieved, q_1 is the probability of success with the first trial. In the general case where damage is in stage j the above probabilities are defined as:

p_j = prob(remain in state|initially in state j) (11)

q_j = prob(pass to the next state|initially in state j)

In the case of ultrasonic monitoring of the elastic constants, the initial dispersion of the experimental values can be assumed to correspond to the damage dispersion for $x = 0$. The probability that damage is in j for DC = 0 is defined as:

π_j = prob {state j is initially occupied} (12)

$\pi_b = 0$

It is obvious that $\Sigma_1^b \pi = 1$. The physical meaning of the assumption that $\pi_b = 0$ is that no specimen is in the failure stage prior to exposure. In this way, the fact that the elastic constants normalized by the asymptotic value, where each distribution is leading, exhibit measurable damage is included in the model. Additionally, "failure" is arbitrarily defined as the maximum measured damage for each exposure.

Recapitulating, the assumptions made for the modeling of the experimental data, that is the experimental cumulative probability functions as presented in fig. 3 are:

1. Loading is discretised in time spans or DC which result to a steady deterioration of the system (stationary model).
2. Damage states are discrete.
3. The deterioration in one DC depends only on the state of the system during the DC and the existing damage at the beginning of the DC.
4. Degradation can only increase during the DC from the already existing damage.

The first assumption is rendering the exposure time discrete, and states that whatever events take place during a DC is also occurring in any DC. The second assumption is rendering discrete damage in allowed damage states. The model does not include the information for whatever is occurring during a DC but only deals with the initial and final damage states. The third assumption is the basic assumption of a Markov process.

The above features can be assembled in a simple mathematical formulation which relates to the calculation of the constant probability transition matrix (PTM) [15]:

$$P = \begin{bmatrix} p_1 & q_1 & 0 & \cdots & 0 & 0 & 0 \\ 0 & p_2 & q_2 & \cdots & 0 & 0 & 0 \\ \vdots & \vdots & \vdots & \cdots & \vdots & \vdots & \vdots \\ 0 & 0 & 0 & \cdots & 0 & p_{b-1} & q_{b-1} \\ 0 & 0 & 0 & \cdots & 0 & 0 & 1 \end{bmatrix} \quad (13)$$

The determination of the PTM is performed through the calculation of the parameters b and r that relate to the mean value μ and variance σ^2 as following:

$$b = 1 + \frac{\mu^2}{\sigma^2 + \mu}$$

and (14)

$$r = \frac{\mu - (b-1)}{b-1}$$

where b corresponds to the final state and $r = p_j / q_j$ [16].

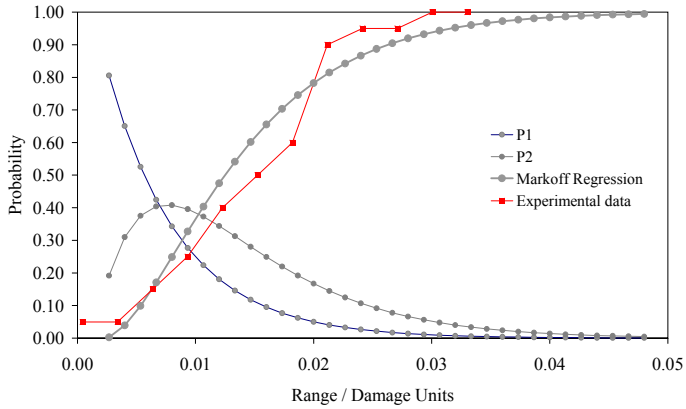

Fig. 5: Markov process modeling for a random observation state

Based on the above, every damage state can be interpolated as a Markov process, as shown in fig. 5, where the Markov process is superimposed on the experimental data at discrete time intervals. The distributions P1 and P2 depict the probability mass transition during the transition in higher damage states which lead to the final distribution that depict the failure probability distribution at the final stage. The Markov process interpolation for various exposure times is shown in fig. 6.

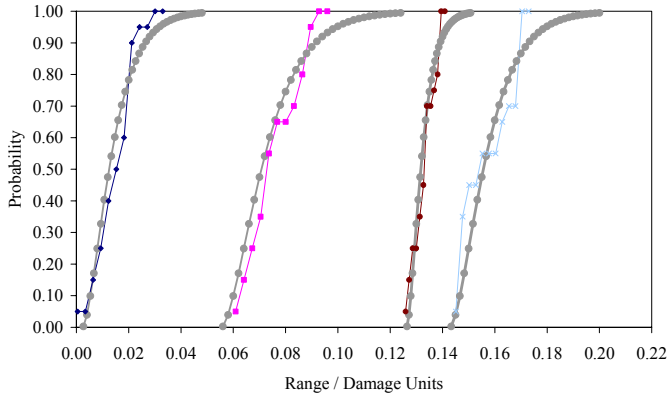

Fig. 6: Markov process modeling for a selection of observation states: probability of failure

4.2.3 Markov Process Simulation

The depiction of selected degradation stages was performed as a Markov process. The total damage evolution can be seen as a Markov process analysed in the degradation axis. However, the general case is concerned with the prediction of the damage evolution of the curves shown in fig. 1. In contrast with the typical damage accumulation process, the following points are made:

1. The damage function is a mean of a series of observations regarding all specimens.
2. The damage function due to the statistical nature of the measurements is not monotonically increasing.

The above statements result from the variability of the level of the critical observation volume of the ultrasonic beam, the experimental error and the numerical error stemming from the inversion algorithm of the scattering problem.
If however we regard the damage accumulation observations as depicted in fig. 1 as Markov processes, then the typical form of the process for a discrete function is given [17]:

$$x_{v+1} = x_v + \kappa\,(\sigma - x_v). \qquad (15)$$

where v are the states of the process as a function of the quantity in interest which in this case is exposure time, κ is the damage increase rate and σ the standard deviation of the measurable quantity x which in this case is an elastic constant.
In order to simulate the degradation process, the stochasticity of the system parameters should be introduced. If we regard an error function with a mean value of U, then the process is simulated as following:

$$x_{v+1} = x_v + \kappa\,(\sigma - \chi_v) + U\,e_{v+1} \qquad (16)$$

where e_{v+1} is a random variable following a normal distribution (0,1). To increase the stochasticity of the process the randomness in the increase rate κ should be introduced, which also has a stochastic nature with an added error function. In this case the damage development is of a stochastic nature regarding the time evolution of the elastic constants of the material. If κ is a known time function, then the model becomes non stationary.

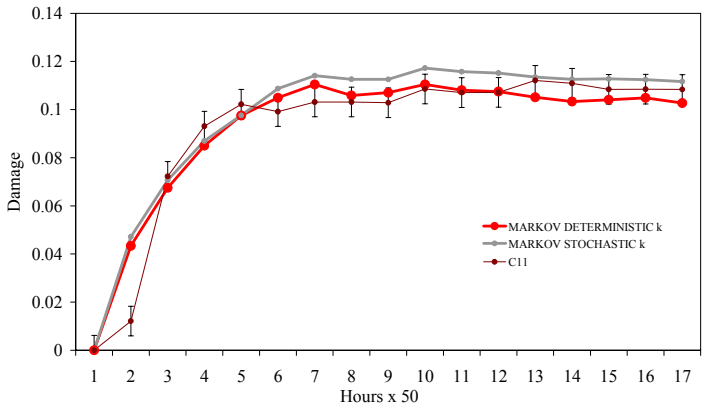

Fig. 7: Markov process simulation for C_{11}

With regard to the above, and using the mean standard deviation value of the deviations observed in the discrete states of damage, the simulation of the damage process for the three measured quantities in the discrete exposure states is shown in figs. 7 and 8 for C_{11} and C_{22} & C_{33} respectively.

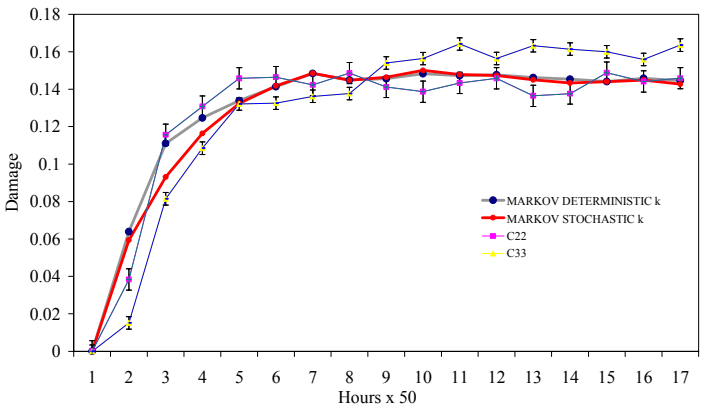

Fig. 8: Markov process simulation for C_{22} and C_{33}

9. CONCLUSIONS

The characterization of composites with non-destructive methods has revealed significant stiffness degradation of the material already from the initial stage of its exposure to 1100 °C. The degradation of stiffness is mainly attributed at the degradation of the mechanical properties of the matrix. The structural changes of the matrix material as well the increase in its porosity, is likely to influence the crack propagation mechanisms during loading. The increase of the pore size decreases the probability of crack diffusion within the matrix, and influences directly the toughness of the material. The observed increase of the grain size of the fibres of the composite, also leads to lower stiffness and strength values as it involves the increase of fault size of the above quantities. These mechanisms should also include the degradation of the fibre / matrix interface [20-21]. Cracking of the fugitive coating allows for sintering of the fibre and matrix across the interface gaps, which also reduces the ability for fibre debonding and pullout. This is consistent to experimental results on the Nextel 720 found in literature. [7]

The ultrasonic method can provide a fairly accurate mean for quantitative stiffness characterisation. In particular, the applied methodology can be considered as a very effective tool during material development stage. The main advantage of the proposed approach, which is based on the developed methodology of the ultrasonic stiffness measurements, is its capacity to follow the evolution of the anisotropic damage and its direct effect on the material properties at various stages of a progressive fermentation, such as oxidation, mechanical and thermal fatigue etc, using a limited number of specimens. Since results are obtained in the form of the complete stiffness matrix of the composite laminate, it is possible to derive equivalent lamina properties, a valuable input for the structural design phase of any components made of laminated materials.

Furthermore, a consistent damage evolution modelling approach was introduced that allows for life prediction analysis of components made of CFCC's under thermomechanical loading. Identification of changes in the material's anisotropy is also possible using a more complicated formulation for the inversion of the phase velocity data. Exponential anisotropic damage functions were developed to describe the deterioration of the composite properties.

A stochastic damage accumulation model was employed using Weibull distributions discrete time Markov chain models to yield service life probability distributions [7]. A Markov process is defined as a process that depends on its current state and its transition to future state and is independent of its past. In this work the stiffness degradation of the material at discrete states is regarded as a Markov process. Finally, a simulation of the stiffness degradation process is presented with varying stochasticity.

ACKNOWLEDGEMENTS

The present work has been performed within the frame of R&D programme BRITE III, 'Ceramic Components for Industrial Gas Turbines - CERCO' of the European Commission. The authors wish to thank the Research Committee of the University of Patras for financial support through the Karatheodoris project and EADS/Dornier GmbH for supplying the used materials.

REFERENCES

1. **Evans, G.** and **Cox, F.W**., "The physics and mechanics of fibre reinforced brittle matrix composites", *J. Mater. Sci*, **29,** (1994), 3857-3896.
2. **Naslain, R**., "Fibre-matrix interfaces and interphases in ceramic matrix composites processed by CVI", *Composite Interfaces*, **1,** (1993), 253-286.
3. **Anson, D**., **Sheppard, W. J.** and **Parks, W. P.**, "Impact of ceramic components in gas turbines for industrial cogeneration", ASME Paper 92-GT-393 International Gas Turbine & Aeroengine Congress & Exhibition, Cologne, Germany, June 1992.
4. **Marshall, D.B.**, and **Davis**, **J.B., "**Ceramics for future power generation: fiber reinforced oxide composites", *Current Opinion in Solid State & Materials Science*, **5**, (2001), 283-289.
5. **Hay, R. S., Boakeye, E., Petry, M.D., Berta, Y., Von Lehmden, K.,** and **Welch**, **K.,** "Grain growth and tensile strength of 3M Nextel 720 after thermal exposure", *Ceram. Eng. Sci. Proc.*, **20**, (1999), 165-172.
6. **Evans, G., Marshall, D.B., Zok, F.,** and **Levi, C.**, "Recent advances in oxide-oxide composite technology", *Adv. Composite Mater.*, **8**, (1999), 17-23.
7. **Kramb, V.A., John, R.** and **Zawada, L.P.**, "Notched fracture behavior of an oxide/oxide ceramic-matrix composite", *J. Amer. Ceram. Soc.*, **82**, (1999), 3087-3096.
8. **Jones, R. E., Petrak, D., Rabe, J.** and **Szweda, A.,** "SYLRAMIC™ SiC fibers for CMC reinforcement*", Journal of Nuclear Materials*, **283-287**, (2000), 556-559.
9. **Johnson, S.M., Blum, Y., Kanazawa, C., Wu, H.-J., Porter, J. R., Morgan, P.E.D., Marshall, D. B.** and **Wilson, D.**, "Processing and properties of an Oxide/Oxide Composite", *Key Engineering Materials*, **127**, (1997), 231-238.
10. **Aristegui, C.**, and **Baste, S.**, "Optimal recovery of the elasticity tensor of general anisotropic materials from ultrasonic velocity data", *J. Acoust. Soc. Am.* **101,** (1996), 813-833.
11. **Nayfeh, A. H.,** "Wave propagation in layered anisotropic media", Elsevier, Amsterdam, 1995.
12. **CEN WI114,** "Determination of elastic properties by an ultrasonic technique", *European Technical Committee*, **184**, (2000).
13. **Baste, S.** and **Audoin, B.**, "On internal variables in anisotropic damage", *Eur. J. Mech., A/Solids*, **10**, (1991), 587-606.
14. **Vlachos, D.E., Paipetis, A. and Kostopoulos, V.**, "Damage accumulation on oxide/oxide composites under thermal exposure", in the Proceedings of Comp 03: Advances in Composite Technology, Corfu, 5-7 May 2003, on CD ROM.
15. **Bogdanoff J. L.** and **Kozin, F.**, "Probabilistic Models of Cumulative Damage", *Wiley*, 1985.
16. **Pappas, Y. Z., Spanos P. D.,** and **Kostopoulos, V.**, "Markov Chains for Damage Accumulation of Organic and Ceramic Matrix Composites", *J. of Eng. Mech.*, **127**, 9, (2001), 915-926.
17. **Papoulis A.**, "Probability, Random Variables and Stochastic Processes", *McGraw-Hill Inc.*, 1991.
18. **Paipetis, A.** and **Kostopoulos, V.**, "Ultrasonic Stiffness Matrix Measurements Of Oxide / Oxide Composites" in Recent Advances in Composite Materials - In honor of S.A. Paipetis, Kluwer Academic Publishers, E. Gdoutos & Z.P. Marioli-Riga (eds), (2003), 167-180.
19. **Ortiz, M.**, "A constitutive theory for the inelastic behaviour of concrete", *Mech. Mater.*, (1985), 67-93.
20. **Peters, P.W.M., Daniels, B., Clemens, F.,** and **Vogel, W.D.**, "Mechanical characterisation of mullite-based ceramic matrix composites at test temperatures up to 1200 ^{o}C", *Journal of the European Ceramic Society*, **20**, (2000), 531-535.
21. **Holmquist, M., Lundberg, R., , Sudre, O., Razzell, A.G., Molliex, L., Benoit, J.** and **Adlerborn, J.**, "Alumina/alumina composite with a porous zirconia interphase - Processing, properties and component testing", *J. of the European Ceramic Society*, **20**, (2000), 599-606.